

LASER-SELECTIVE CHEMISTRY AND VIBRATIONAL ENERGY REDISTRIBUTION IN MOLECULES*

AHMED H. ZEWAİL

Arthur Amos Noyes Laboratory of Chemical Physics, California Institute of Technology, Pasadena, CA 91125 (U.S.A.)

Summary

I present new experimental results that are relevant to how vibrational energy is redistributed in large molecules. In these experiments the molecules are cooled (by supersonic beam expansion or by low temperature (1.7 K) crystal techniques) and the vibrational states are excited *selectively* by optical pulses of approximately 15 ps duration. When combined with high resolution spectroscopic data, the results of these experiments tell us the energy and phase relaxation time scales. The relevance of these and other findings to laser-selective chemistry is discussed.

1. Introduction

Photochemistry by lasers is a subject of great current interest. Of particular interest is the randomization of *energy* and *phase* among the large number of vibrational states at high energies following the selective and well-defined excitation by the laser to a specific state. Knowledge of these randomization rates and the rates of chemical reactions involving these large molecules tells us whether or not laser-selective chemistry is possible. If on the time scale of the experiment vibrational energy redistribution is complete among the vibrational modes, then we use the statistical theories, such as the Rice–Ramsperger–Kassel–Marcus theory (RRKM), to describe the chemical changes. If, however, the vibrational energy redistribution is non-statistical, then we may be able to localize energy selectively in certain modes.

With the advances made in the development of ultrashort-time laser pulses (picosecond to subpicosecond) and ultrahigh frequency resolution (megahertz to kilohertz) some of the following dynamical questions pertinent to the above-mentioned problems can perhaps now be answered.

(a) What is the nature of the state that we excite with light? Is it a *local* or a *normal* mode of the system?

(b) How can we separate the different intramolecular channels that lead to randomization?

* Paper presented at the Xth International Conference on Photochemistry, Iraklion, Crete, Greece, September 6 - 12, 1981.

(c) What determines dephasing and energy relaxation in large molecules?

In the following sections, I shall describe how some laser techniques can be used to probe the dynamics of intramolecular energy and phase redistributions, as outlined in the above questions. First, however, a brief description of dephasing in two-level and multilevel systems will be given.

2. Optical phase and energy redistribution

2.1. The two-levels–bath problem

Here we shall consider the interaction of two quantum states in contact with a bath to a laser field. To describe the origin of optical dephasing in such a system we shall consider only the semiclassical approach—the molecule is treated quantum mechanically and the laser field classically. Semiclassically, we describe the process as follows: the laser field E interacts with an ensemble of molecules to produce a time-dependent polarization $P(t)$, which in turn changes as the molecules dephase. So, our task is to find how the polarization is related to dephasing and what dephasing means on the molecular level.

Consider two vibronic states: a ground state $\psi_a(r)$ and an excited state $\psi_b(r)$. The laser field is simply a wave (propagation direction, z) of the form

$$E(z,t) = \varepsilon \cos(\omega t - kz) = \frac{1}{2}[\varepsilon \exp\{i(\omega t - kz)\} + \varepsilon \exp\{-i(\omega t - kz)\}] \quad (1)$$

where ε is the amplitude and ω is the frequency of the radiation. The state of the molecule (driven by the laser) at time t may be represented as

$$\psi(r,t) = a(t) \exp(-i\omega_a t) \psi_a(r) + b(t) \exp(-i\omega_b t) \psi_b(r) \quad (2)$$

We now can calculate the time-dependent molecular polarization:

$$\begin{aligned} P_m(t) &= \langle \psi(r,t) | \hat{\mu} | \psi(r,t) \rangle \\ &= ab^* \mu_{ba} \exp\{-i(\omega_a - \omega_b)t\} + a^*b \mu_{ab} \exp\{-i(\omega_b - \omega_a)t\} \end{aligned} \quad (3)$$

where $\hat{\mu}$ is the dipole moment operator and μ_{ba} and μ_{ab} are the transition moment matrix elements. Taking these matrix elements to be equal ($\equiv \mu$) and setting $\omega_b - \omega_a = \omega_0$ (the transition frequency) we obtain

$$P_m(t) = \mu \{ ab^* \exp(+i\omega_0 t) + a^*b \exp(-i\omega_0 t) \} \quad (4)$$

Hence the polarization, which is related to the radiation power, is zero if there is *no* coherent superposition or, in other words, if the molecule is certain to be in the state a or b . From eqn. (4) the total polarization for N molecules in the sample (assuming equal contributions and ignoring propagation effects) is therefore

$$P(t) \equiv \frac{1}{2} \{ \bar{P} \exp(i\omega_0 t) + \bar{P}^* \exp(-i\omega_0 t) \} = N\mu(\varrho_{ab} + \varrho_{ba}) \quad (5)$$

where $P(t) \equiv NP_m(t)$ and \bar{P} is its complex amplitude, *i.e.* $\bar{P} = \bar{P}_{\text{real}} + i\bar{P}_{\text{imag}}$. We chose the notation ϱ_{ab} and ϱ_{ba} for the cross-terms $ab^* \exp(+i\omega_0 t)$ and

$a^*b \exp(-i\omega_0 t)$ because they are indeed the off-diagonal elements of the ensemble density matrix ρ . Equation (5) shows that in order to create a polarization or optical coherence we need a non-vanishing interference term or equivalently the off-diagonal elements of ρ must be non-zero in the zero-order basis set.

From eqn. (2) we see that the probability of finding the system in the excited (ground) state is simply $|b|^2$ ($|a|^2$). These probabilities decay by time constants, say T_{1b} and T_{1a} respectively. Such phenomenological decay is the result of the Wigner–Weisskopf approximation, *i.e.* an exponential decay of the amplitudes a and b ; $a \propto \exp(-t/2T_1)$ or $b \propto \exp(-t/2T_1)$. Also, the cross-terms of eqn. (2) will decay possibly at a different rate from the diagonal terms. This decay constant is T_2 or the dephasing time and is given by [1]

$$\frac{1}{T_2} = \frac{1}{T_2'} + \frac{1}{2} \left(\frac{1}{T_{1a}} + \frac{1}{T_{1b}} \right) \quad (6)$$

The T_1 term in eqn. (6) comes from the diagonal elements and represents an average rate for the loss of population in the ab levels. Physically, the T_2' term represents the additional decay caused by phase changes in the cross-terms. In other words, the *random* and rapid variation in the transition frequency $\omega_0(t)$ causes the off-diagonal elements to decay faster than the diagonal ones. It can be shown that the linewidth of the transition $a \rightarrow b$ is $1/\pi T_2$ if the band profile is lorentzian. The *total* dephasing rate is therefore $1/T_2$; it contains $T_2'^{-1}$ (the rate for phase coherence loss (pure dephasing)) and T_1^{-1} (the rate for irreversible loss of population (energy relaxation or randomization in the two levels)). The phenomenology described here is the optical analog of the magnetic resonance T_1 and T_2 of Bloch's equation, but the physics is different.

2.2. Bath-independent dephasing in multilevel systems

It is desirable to use laser pulses that make the coefficients in eqn. (2) equal (the $\pi/2$ pulse limit). In a macroscopic system a single $\pi/2$ pulse might excite 10^{18} molecules, each of which is coupled to some extent to all others. In large molecules, such excitation and coupling cannot be handled in a manner similar to that of the two-level limit we described before. This is simply because the eigenstates of such a system are very difficult to ascertain. Warren and Zewail [2] have recently used the method of moments to obtain expressions for dephasing in multilevel systems. We considered two-level "subsystems" coupled together by an interaction hamiltonian (*e.g.* the dipole–dipole interaction) to produce the real system that we excite with light. Unlike the two-level case where the pure dephasing rate goes to zero at zero temperature, the multilevel system case shows a non-zero dephasing even at 0 K. The implications of these findings for *isolated* large molecules with overlapping resonances are very important.

3. Experimental probing of dephasing and energy randomization

3.1. Two-level molecules in bulbs and beams

Laser techniques are now available to separate directly optical (T_1 and T_2), energy and phase relaxation time constants (for a review, see ref.1). In

diatomic molecules, which approximate the two-level limit very well, this has been demonstrated experimentally. In Fig. 1 we depict the coherent transients [1] obtained by using a continuous-wave (CW) laser and switch. A single-mode laser (width, less than 5 MHz) is used to excite coherently a homogeneous subgroup of molecules. The laser is then either diffracted acoustically so that it

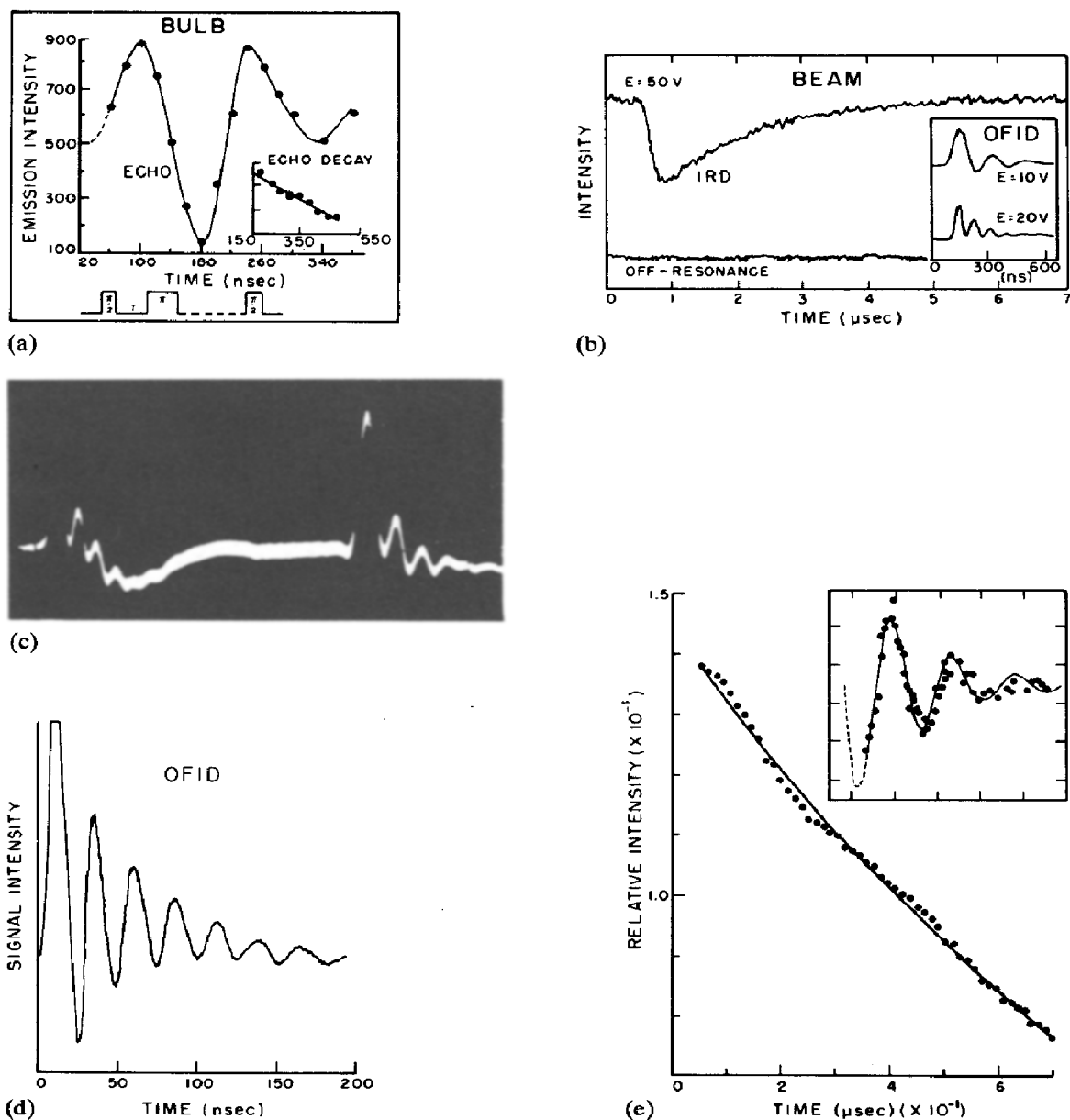


Fig. 1. The different coherent transients observed in gases and beams of iodine [1]: (a) photon echo; (b) the incoherent resonance decay and free induction decay (FID) in an iodine beam; (c), (d) FID of I_2 gas; (e) nutation. For details see ref. 1 and references therein.

will no longer "see" the sample or switched into another frequency within the optical line. The $\pi/2$ and π pulses are made by controlling the diffraction duration time or the frequency-switching time. Details can be found in refs. 1 and 3.

When a group of molecules are excited coherently the superposition of states discussed before will be established. As a result, a polarization is induced and, if for example the laser is immediately turned off, a coherent burst of light, sometimes called superradiance [4], can be detected. Several transients [1, 3, 5, 6] can be observed depending on the pulse sequence. These include photon echo, optical nutation, incoherent resonance decay and optical free induction decay (OFID). Using the *incoherent* spontaneous emission, all these coherent transients have been observed (for a review see refs. 1 and 3). The important point is that from the transients we can obtain T_1 , T_2 and μ , as detailed elsewhere [1].

3.2. Large molecules in bulbs, beams and solids

The optical dephasing time for the diatomic I_2 has been measured directly in a collisionless beam [7]. So far direct T_2 measurement for larger molecules has not been reported. However, many experiments have been performed to infer processes causing redistribution. Among these are (i) fluorescence as a function of excitation energy of molecules in bulbs, (ii) fluorescence and excitation spectra of molecules in supersonic beams, (iii) intracavity absorption of molecules in supersonic beams, (iv) time-resolved fluorescence of molecules in bulbs, (v) collision-induced fluorescence changes of molecules in bulbs, (vi) picosecond spectroscopy of molecules in supersonic beams and (vii) line shape analysis of high energy vibrational transitions.

Many groups, especially the group of Lim at Wayne State University, have investigated (i) and have projected the effect of excess energy on randomization. One of the problems with this type of experiments is the thermal congestion. In other words, because the experiments are done at room temperature the thermal energy is quite high and is "carried up" to the excited state, resulting in a "contaminated" and ill-defined excitation. In recent years the supersonic cooling method pioneered by Levy *et al.* (University of Chicago), Smalley *et al.* (Rice University) and Jortner *et al.* (Tel Aviv University) has been used (for a recent review, see ref. 8) to solve this problem and to infer the dynamics from the CW spectra. Parmenter's group at Indiana University have monitored carefully the fluorescence of *p*-difluorobenzene as a function of buffer gas pressure and inferred the dynamics at "zero pressure" in the bulb [9]. Tramer *et al.* in France and Langlaar *et al.* in Holland time resolved the fluorescence but again for molecules in a bulb with definite thermal energy [10]. These experiments give different redistribution times: 10 ps and 0.3 ns.

Our own effort at Caltech has been focused around (a) the time and frequency resolution of fluorescence of large molecules in supersonic beams and excited by 15 - 20 ps pulses, (b) line shape analysis of high energy vibrational overtone states in solids at 1.7 K and (c) intracavity absorption of rotationally and vibrationally cooled molecules.

In what follows I shall describe briefly these techniques and discuss the new findings.

4. High energy vibrational overtone spectra of large molecules: vibrational dephasing and the state excited

In recent years, there has been much interest in the nature of vibrational states of molecules at high energies. The important problems in this field are centered around the following questions.

(a) Is the excitation in the high energy states localized or delocalized?

(b) What is the time scale for vibrational energy redistribution?

(c) What is the relevance of these states and their relaxation to possible mode-selective chemistry?

Overtone spectroscopy, including direct absorption and emission, thermal lensing and photoacoustic spectroscopy, has been the primary experimental technique used to obtain information in attempts to answer these questions. The spectra of X-H-stretching overtones obtained in liquids, gases and solids have been consistent with the local-mode model in which the vibrational excitation is considered to be localized in certain bonds (for a review, see ref. 11). Also, from spectral bandwidths (typically 100 cm^{-1}), relaxation times for these high energy ($\Delta v = 5, 6, 7, \dots$) overtone states were inferred to be approximately 100 fs or shorter. The locality of excitation was inferred from the success of applying the simple diatomic formula $E(v) = Av + Bv^2$, where v is the vibrational quantum number of the CH stretches, in many polyatomic molecules.

In Fig. 2 we present the low temperature (less than 2 K) $\Delta v = 5$ CH-stretching absorption spectrum of durene and durene- d_2 . The first feature we wish to point out is the absence of the broad band at $\Delta \bar{\nu} \approx 900\text{ cm}^{-1}$ ($\lambda = 7209\text{ \AA}$) in the durene- d_2 spectrum and the qualitative consistency of the remaining features of the spectrum. On this basis we assign the band at 7209 \AA as the aromatic $\Delta v = 5$ CH-stretching mode. The other bands around $\Delta \bar{\nu} = 300 - 600\text{ cm}^{-1}$ ($\lambda \approx 7400\text{ \AA}$) are methyl-based CH-stretching modes.

In the region of the methyl CH-stretching modes, the linewidths of the bands vary from 20 to 50 cm^{-1} , different from the 100 cm^{-1} of the aromatic. The methyl CH-stretching mode bandwidths are the smallest bandwidths yet observed in high energy overtone spectra of polyatomic molecules. The small widths of the methyl bands imply that these modes relax more slowly than the

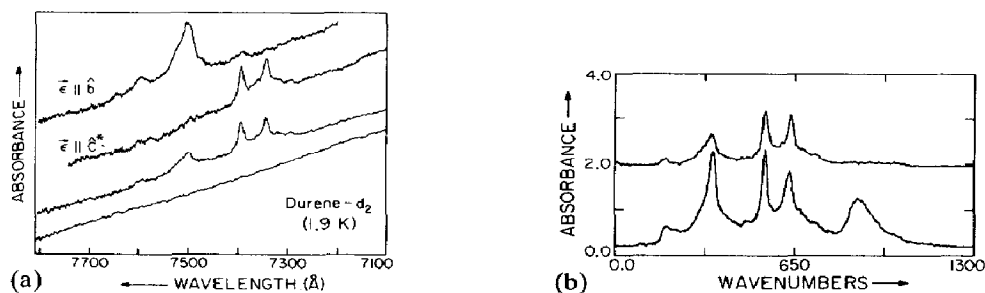


Fig. 2. (a) Low temperature (less than 2 K) CH-stretching $\Delta v = 5$ overtone spectra of durene and durene- d_2 crystals. The absorbance is in arbitrary units and the horizontal scale is in unit change from $12\,990\text{ cm}^{-1}$. (b) The polarization spectra of the same bands of durene- d_2 .

aromatic CH-stretching modes. Provided that pure dephasing is negligible, this can be explained as a larger population relaxation time constant for the methyl CH-stretching modes. The slower relaxation of the methyl modes makes sense qualitatively since there is a C–C bond separating the methyl CH bonds from the benzene ring (bath). This separation reduces the average potential or kinetic energy coupling of methyl CH-stretching modes to the ring modes relative to the aromatic analogue.

The narrowness and the large spectral splittings of the aliphatic bands relative to the aromatic band lead us to consider two important points: (a) there are two distinct types of relaxation of the different CH modes to other modes within the molecule and (b) the states prepared optically are different in nature for the aliphatic and aromatic CH modes. The vibrational relaxation problem here is strongly connected with the problem of vibronic or electronic relaxation as pointed out by Sage and Jortner [12].

In the intermediate coupling case, the states prepared with narrow-band excitation are non-stationary (*i.e.* have finite width) because of interactions with the manifold of bath modes, but the states of the “optically active” manifold (at a given quantum level) are separated by an amount Δ which is larger than the corresponding linewidths W ; thus $W/\Delta < 1$ and we are able to resolve the individual “eigenstates” approximately. Since for the aliphatic CH subset of modes $W/\Delta \approx 0.2 - 0.1$, the modes should belong to the intermediate-coupling case and should exhibit distinct polarization characteristics (Fig. 2). For the usual aromatic CH-stretching modes (*e.g.* benzene), the linewidths are broad (of the order of 100 cm^{-1}) and the spacing of the states is small ($W/\Delta \gtrsim 1$). Thus, we can excite only a superposition of symmetry-adapted states leading to localization of the excitation. In this sense, the aromatic CH-stretching modes belong to the statistical limit and correspond approximately to local modes with ultrashort lifetimes (femtoseconds). More details can be found in ref. 11.

In conclusion, our observations suggest that relatively slow intramolecular CH-stretching relaxation ($\tau = 0.5 \text{ ps}$ in contrast with the 0.075 ps of the aromatic mode) in sizable molecules such as durene (24 atoms) is possible at high energies ($\Delta\nu = 5$). Also, the polarized absorption spectra lead to interpretation in terms of symmetry-adapted states for the aliphatic CH-stretching modes. The interplay between spectral splittings and linewidths determines the nature of the vibrational state excited. We are currently considering the polarization data of other possible conformers of durene to ascertain more positively the assignment (pure local modes *versus* interacting local modes).

5. Intracavity absorption of molecules in supersonic beams

Recently we reported [13] on the observation of intracavity absorption of the photochemically active molecule dimethyl-*s*-tetrazine (DMT) in a supersonic beam. The rotational and vibrational temperatures were less than 0.1 K and 16 K respectively. Under these conditions, the cooled molecules were excited to the different overtones of the 520 cm^{-1} mode during detection of the fluorescence or the transmitted beam (Fig. 3). We find that the absorption and excita-

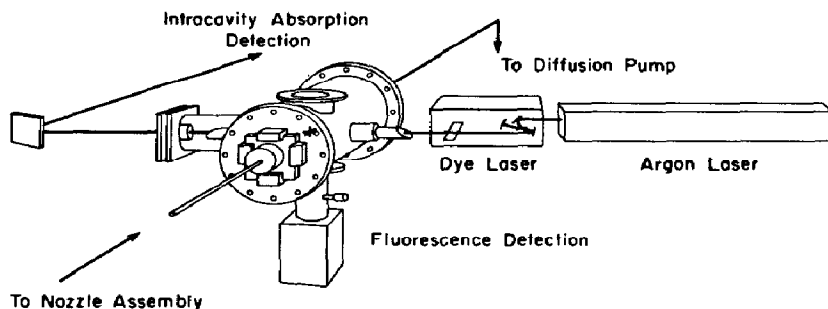


Fig. 3. The experimental arrangement for intracavity absorption spectroscopy in a molecular beam.

tion spectra are different as a result of the large quantum yield for photochemistry. In this low energy region the dissociation of the molecule is selective but the quantum yield is non-monotonic with energy. The dissociation behavior in the high excess energy region (more than 3000 cm^{-1} above the origin of S_1) is still unknown.

6. Time-resolved spectroscopy of molecules in supersonic beams: excitation with picosecond pulses

Recently, Lambert and Felker of Caltech have observed time-resolved and frequency-resolved spectra of anthracene in a supersonic beam using pulses of 15 - 20 ps duration. The fluorescence, which exhibits *quantum beats*, was detected with a medium resolution spectrometer and detection system capable of 50 ps resolution. The laser was tuned to the different 1400 cm^{-1} modes which are optically active in absorption and emission.

In Fig. 4 we show spectra of anthracene cooled by supersonic expansion with neon, helium or argon. We also show the decay characteristics at different energies. Several interesting observations are noteworthy. Firstly, the lower spectrum D is considerably sharper than spectrum B, although both resulted from anthracene excited at about $31\,900\text{ cm}^{-1}$. In addition, the fluorescence decay characteristics of the two spectra are different. These discrepancies can only be attributed to a difference in the nature of the molecular beams being excited. Secondly, there are two trends in the spectra as the excitation energy is systematically changed. With increasing excitation energy, the emission broadens and shifts to the red. Thirdly, for excitation at $33\,300$, $31\,900$ and $30\,550\text{ cm}^{-1}$, the fluorescence lifetime observed is dependent on the frequency of the emission collected. To the red of $28\,000\text{ cm}^{-1}$ in spectra B and C, there is a small systematic decrease in the lifetime as the energy of emission decreases. In addition, the weak emission at about $30\,550\text{ cm}^{-1}$ in spectra A and B is very long compared with the bulk of the emission. Lastly, there is a slight trend toward shorter lifetimes as the excitation energy increases. Pending more detailed experimentation, we have made the following preliminary interpretations of the data.

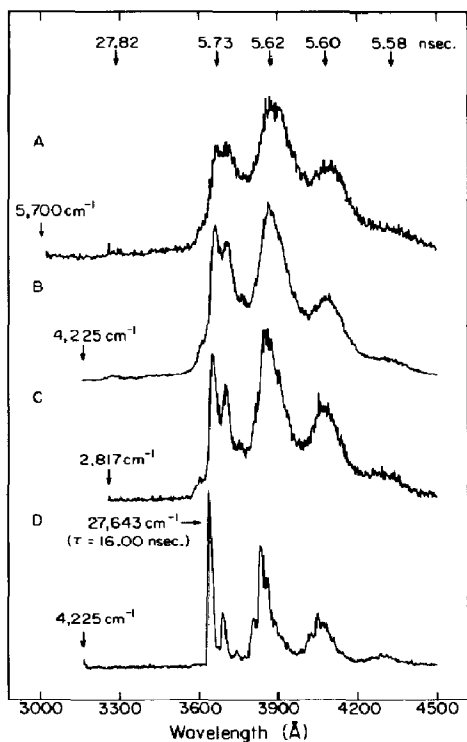


Fig. 4. Molecular (supersonic) beam spectra of anthracene at different excitation energies. The excess excitation energy is denoted by an arrow and the fluorescence origin is indicated by the vertical line. The lifetimes at the top are obtained by time resolving the fluorescence spectrum A at different energies. Typical beam conditions (A and B) are as follows: back pressure of neon, 75 lbf in⁻²; nozzle diameter, 150 μ m; laser-nozzle distance, about 7 mm; nozzle temperature, 180 °C.

Consider first the nature of the emitting state, which gives rise to spectrum D. On excitation at 31 900 cm^{-1} , anthracene is prepared with about 4200 cm^{-1} of vibrational energy in the S_1 electronic state. If this excitation process takes place in a region of a supersonic molecular beam where cooling collisions occur readily, then relaxation of the optically prepared state to lower energy vibrational states of S_1 might be expected. We believe that spectrum D is emission from excited anthracene molecules that have been collisionally cooled to the lowest energy vibrational state of S_1 . Several facts support this conclusion.

(1) Spectrum D was collected under conditions wherein the laser excitation beam crossed the molecular beam at a point close to the supersonic nozzle source. As the distance between the two increased, the sharpness of the spectrum decreased.

(2) There is a measurable rise time (about 1 ns) to the emission at 27 650 cm^{-1} under the conditions at which spectrum D was taken. This is consistent with a time-dependent process occurring after excitation and leading to population of the emitting state. Note that such slow rise times are not observed for the

other bands of the spectrum. Presumably this difference is due to the fact that the optically prepared state does not emit strongly at $27\,650\text{ cm}^{-1}$, while it does so to the red of this (*cf.* the red shift of anthracene fluorescence with increasing excitation energy).

(3) The approximate lifetime of the emission (16 - 20 ns) is consistent with previous measurements of the fluorescence lifetime on excitation of the S_1 origin.

(4) Within experimental error, the strongest peak occurs at the energy of the S_1 origin. Moreover, there is no structure to the blue of this peak, indicating that the emitting state is the zero-point vibrational level of S_1 . The "filling" of the spectra as the excitation energy increases suggests an increase in the rate of dephasing, even though the lifetime or the T_1 -type relaxation is essentially unchanged. Although it seems clear that initially rapid dephasing takes place in anthracene at excitation energies of more than about 2800 cm^{-1} above the S_1 origin, the data also suggest that once this process has taken place further redistribution occurs on a time scale that is comparable with the fluorescence lifetimes of the S_1 states. We infer this from the fact that lifetimes for a given excitation energy depend on the frequency of the fluorescence that is collected. If there were rapid "communication" among all the states having a given vibrational energy excess, we would expect a constant lifetime as we tuned across the emission spectrum. Excess vibrational energy is evident from the real red shift observed for high excitation energies.

Consistent with this picture is the appearance of the weak hot band at about $30\,550\text{ cm}^{-1}$. Although its assignment is not unequivocal at the moment we have, nevertheless, several reasons to believe that the data are real. Firstly, the lifetimes are very reproducible. Secondly, the $30\,550\text{ cm}^{-1}$ band occurs at 2800 cm^{-1} above the S_1 origin and is consistent with emission characterized by $\Delta\nu = -2$ involving the optically active 1400 cm^{-1} mode. Moreover, similarly long-lived emission also occurs at 1400 cm^{-1} above the origin. Finally, control experiments have been performed to verify that all the observed fluorescence is due only to excited species in the molecular beam.

With all these results in mind, we are led to the following picture of anthracene decay dynamics. Excitation of cool isolated anthracene at $30\,550\text{ cm}^{-1}$, $31\,900\text{ cm}^{-1}$ and $33\,330\text{ cm}^{-1}$, corresponding to initial populations of 2, 3 and 4 quanta respectively in the optically active 1400 cm^{-1} mode, is followed by very rapid intramolecular vibrational energy dephasing into S_1 vibrational states of the form $|I, \{n\}_J\rangle$, where I is the number of quanta in the 1400 cm^{-1} mode and $\{n\}_J$ represents a distribution of quanta over all the other vibrational modes of the molecule. Assuming that this redistribution populates all possible states with roughly equal probability, then relaxed states of the form $|0, \{n\}_J\rangle$ will be much more numerous than states $|1, \{n\}_K\rangle$, which will be more numerous than states $|2, \{n\}_L\rangle$ etc. This follows from a density of states argument. Since the emission spectra of these ensembles of relaxed states will reflect the population distributions of emitting states, it is easy to see why the emission at $30\,550\text{ cm}^{-1}$ in spectra A and B (which can be attributed to $|2, \{n\}_L\rangle$ states) is so much weaker than the bulk of the emission, which occurs to the red of the origin and is attributable to emission from $|0, \{n\}_J\rangle$ states.

Following the initial energy dephasing, the relaxed states undergo limited coupling with one another, *i.e.* the decay of a given state is not entirely determined by further vibrational energy redistribution. As a result, each state makes an individual contribution to the overall temporal and spectral characteristics of the fluorescence. For example, the emission decay at $30\,550\text{ cm}^{-1}$, on $31\,900\text{ cm}^{-1}$ excitation, reflects in this scheme the decay properties of the $|2, \{n\}_K\rangle$ emitting states. In contrast, the time-resolved fluorescence at $26\,000\text{ cm}^{-1}$ after similar excitation reflects the decay characteristics of predominantly $|0, \{n\}_J\rangle$ states. Any difference in the two decays is due to differences in their individual coupling to the various radiative and non-radiative electronic decay pathways.

Acknowledgment

This material is based upon work supported by the National Science Foundation under Grants DMR8105034 and CHE7905683.

References

- 1 A. H. Zewail, *Acc. Chem. Res.*, **13** (1980) 360, and references therein.
- 2 W. Warren and A. H. Zewail, *J. Phys. Chem.*, **85** (1981) 2309.
- 3 T. E. Orlowski and A. H. Zewail, *J. Chem. Phys.*, **70** (1980) 1390, and references therein.
- 4 M. Sargent III, M. Scully and W. Lamb, Jr., *Laser Physics*, Addison-Wesley, Reading, MA, 1979.
- 5 R. G. Brewer and A. Genack, *Phys. Rev. Lett.*, **36** (1976) 959.
- 6 T. J. Aartsma, J. Morsink and D. Wiersma, *Chem. Phys. Lett.*, **47** (1977) 425.
- 7 A. H. Zewail, T. Orlowski, R. Shah and K. E. Jones, *Chem. Phys. Lett.*, **49** (1977) 520; *J. Chem. Phys.*, **69** (1978) 3350.
- 8 A. Amirav, U. Even and J. Jortner, *J. Chem. Phys.*, **74** (1981) 3745, and references therein.
- 9 R. Coveleskie, D. Dolson and C. Parmenter, *J. Chem. Phys.*, **72** (1980) 5774.
- 10 N. Halberstadt and A. Tramer, *J. Chem. Phys.*, **73** (1980) 6343.
- 11 J. Perry and A. Zewail, *J. Phys. Chem.*, **85** (1980) 933, and references therein.
- 12 M. Sage and J. Jortner, *Chem. Phys. Lett.*, **62** (1979) 451.
- 13 Wm. Lambert, P. M. Felker and A. H. Zewail, *J. Chem. Phys.*, **74** (1981) 4732.